

Journal of Materials Chemistry B

Accepted Manuscript



This is an *Accepted Manuscript*, which has been through the Royal Society of Chemistry peer review process and has been accepted for publication.

Accepted Manuscripts are published online shortly after acceptance, before technical editing, formatting and proof reading. Using this free service, authors can make their results available to the community, in citable form, before we publish the edited article. We will replace this *Accepted Manuscript* with the edited and formatted *Advance Article* as soon as it is available.

You can find more information about *Accepted Manuscripts* in the [Information for Authors](#).

Please note that technical editing may introduce minor changes to the text and/or graphics, which may alter content. The journal's standard [Terms & Conditions](#) and the [Ethical guidelines](#) still apply. In no event shall the Royal Society of Chemistry be held responsible for any errors or omissions in this *Accepted Manuscript* or any consequences arising from the use of any information it contains.

Cite this: DOI: 10.1039/c0xx00000x

www.rsc.org/xxxxxx

PAPER

Diffusion properties of inkjet printed ionic self-assembling polyelectrolyte hydrogels

Skander Limem,^{*a} and Paul Calvert^b

Received (in XXX, XXX) Xth XXXXXXXXX 20XX, Accepted Xth XXXXXXXXX 20XX

DOI: 10.1039/b000000x

In the present work, Crank's model was used to characterize solute transport in inkjet printed polyelectrolyte gels. The diffusion of a small charged molecule (fluorescein), various size linear uncharged molecules (dextrans), and a globular protein (albumin) in printed PSS-PDDA with near stoichiometric composition happened respectively at about 10^8 , 10^9 , and 10^{10} cm²/sec. Polyelectrolyte complexes printed with non-stoichiometric ratios were found to be non-equilibrium structures consisting of three populations of polymer chains: fully complexed chains, chains in partial electrostatic interaction with the complex, and chains in excess having minimal interaction with the complex. This structure may be multiple phases. The applicability of hydrodynamic and free volume models to describe transport in printed polyelectrolyte gels was discussed.

Keywords

Polyelectrolyte, hydrogel, inkjet printing, transport, diffusion

Introduction

The developing interest in tissue engineering has also exposed a need for gels with good mechanical properties that also allow rapid diffusion of metabolites and signaling proteins. Unlike many synthetic gels used in tissue engineering, extra-cellular matrix is a highly ionized, multi-phase structure. Ionic self-assembled polyelectrolytes, also known as polyelectrolyte multilayers (PEMs), have developed into exceptional biomaterials due to the high degree of molecular control over the film architecture and thickness, the ability to integrate bioactive molecules without losing their functionality, and the simple process to make these thin films¹. The most widespread techniques to make PEMs are dip-coating², spin-coating^{3,4}, and spraying⁵. Despite their versatility and sub-nanometer control level, these techniques require a homogenous and smooth substrate, specific surface chemistry, expensive equipment, sequential washing, and long adsorption times⁶. It would take weeks to make two millimeter thick films using the traditional dipping method⁴. To accelerate the fabrication process, spin coating has been optimized and the same thickness was achievable in less than a day⁷.

More recently inkjet printing was proposed as a rapid and controllable way to make ionic self-assembled polyelectrolytes

with the ability to make patterns on a wide variety of substrates^{8,9}. Previous work has shown that print settings and ink concentrations can be adjusted to form micrometer thick gels in less than an hour⁸. This formation speed and the flexibility of the substrate type make ionic self-assembling polyelectrolyte gels an appealing scaffold system for simultaneous printing with living cells for tissue engineering applications.

To evaluate the suitability of a given hydrogel for tissue engineering applications, it is critical to understand how nutrients, waste products, gasses and bioactive agents are exchanged within it. To do so, a common approach has been to determine the diffusion coefficients of well characterized solutes by measuring their release rate from the hydrogel of interest. Solute transport in hydrophilic gels can be categorized based on the rate-limiting step for their controlled release such as: diffusion, swelling, or chemically-controlled¹⁰. Swelling-controlled release (Case II transport), takes place when the diffusion of the solute is faster than hydrogel swelling. Diffusion-controlled release (Case I transport) is by far the most widely applicable mechanism¹⁰⁻¹². In order to identify the solute transport mechanism in a given hydrogel system, the most frequently used semi-empirical method^{12,13} is the so called 'power rule' developed by Ritger-Peppas for non-swelling gels under perfect sink conditions¹⁴. Except in hydrogels with large pores (> 0.1 μm) or forced flow conditions, solute transport through hydrogels is primarily driven by Fickian diffusion rather than convection¹¹. Crank's model is the solution of Fick's law applied to a homogenous distribution of a given solute in a gel matrix, also referred to as 'monolithic solution in a matrix system' with a 'slab' geometry^{15,16}. This model can predict the diffusion of a wide range of solutes including small molecular weight drugs and biomacromolecules like proteins¹⁷ and DNA¹⁵. Fickian diffusion is applicable in most gels provided that their structure is primarily amorphous and homogenous¹⁸. Fickian analysis is, however, inadequate if the gel is significantly heterogeneous¹⁹ with regard to structural discontinuities (e.g. localized crystallization or phase separations), non-swollen glassy regions (large size gels with slow water diffusion),²⁰ interpenetrating structures,²¹ or composite formations (such as fibrous inclusions).^{22,23}

The aim of this paper is to characterize transport in slow printed polyelectrolyte gels and discuss the applicability of the commonly used free volume²⁴ and hydrodynamic²⁵ transport theories to these printed ionic self-assembling gels. To do so, the release profile of a small charged molecule (fluorescein), various

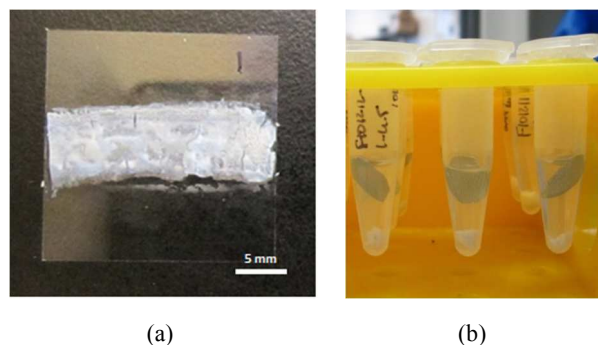


Figure 1. Experimental setup to measure solute release in 1X PBS at physiological pH. (a) Printed PSS-PDDA gel on glass substrate, and (b) after adding 1X PBS and metal mesh to prevent debris pick up during sampling.

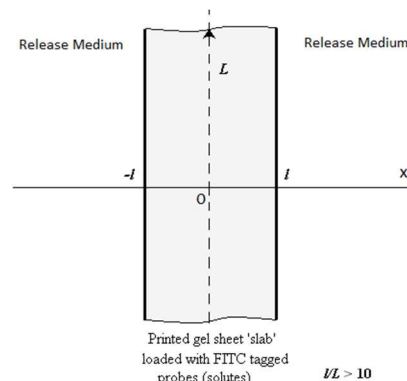


Figure 2. Plane sheet 'slab' configuration.

size linear uncharged molecules (dextrans), and a globular protein (albumin) from printed gels of poly(sodium 4-styrene sulfonate) (PSS) and poly-(diallyl dimethyl ammonium chloride) (PDDA) were measured under physiological conditions. Crank's model was then applied to calculate diffusion coefficients²⁶. The mixture ratio of anion to cation was varied to evaluate the effect of stoichiometry on transport in printed polyelectrolyte gels. In addition to shedding light on the suitability of polyelectrolyte gels in tissue engineering, the measured diffusion coefficients will prove useful in designing tunable drug delivery systems and selective protein filters for immunoassay applications.

Experimental

Ink preparation

Aqueous solutions of PSS with average molecular weight (M_w) ~70,000 g mol⁻¹ (Aldrich, USA) and PDDA with $M_w < 100,000$ g mol⁻¹ (Aldrich, USA) were prepared by dilution with Milli-Q water (18.2 MΩ/cm) from as-received PSS (powder form) and PDDA (40% w/v), respectively. The final polymer concentration for both PDDA and PSS in the ink solutions before printing was 1.0% w/v. Solute molecules used in the diffusion experiments were added to each polyelectrolyte ink to trap solute molecules uniformly throughout the printed gel thickness. Solute concentrations were such that the solute amount at time $t = 0$ is equal or less than 3 % of the printed gel's dry weight. Solutions were filtered with a 0.5 mm filter before loading them in cartridges.

Sample Gel printing

PSS-PDDA gel samples were formed on glass cover slips using the slow print settings on the IIS 56 printing system (Imtech, USA) described in our previous work⁸. The print frequencies for each ink were selected to reach the target anion / cation mixture ratios. Samples were made in a rectangular shape 6.5 mm wide by 22 mm long as shown in Figure 1. The thickness, used in the diffusion studies, of wet printed gels were measured using a KH-7700 3D digital light microscope.

Diffusion characterization

Solutes

The solute release from printed PSS-PDDA gels was measured in 1X PBS at 37°C to determine their diffusion rates under physiological conditions. Different size solutes were chosen to

represent the size range of compounds essential to cell viability and function. The ratio of positive to negative charged polymers in printed PSS-PDDA gels was also varied to evaluate the change, if any, of the diffusion rates.

Fluorescein (332 Da, Sigma-Aldrich, MO, USA) was used as a solute model for small negatively charged molecules at physiological pH. *Dextran* solutes tagged with fluorescein isothiocyanate (FITC) were used as a solute model for linear uncharged molecules. Four molecular weights were tested: 10k, 40k, 150k, and 250kDa (Sigma-Aldrich, MO, USA). *Albumin* (67 kDa), a ubiquitous serum protein, tagged with FITC (Sigma-Aldrich, MO, USA) was used as a solute model for globular molecule negatively charged at neutral pH (isoelectric point = 4.7).

Release profile measurement

The solute release profile was established by measuring the concentration of solutes in the supernatant surrounding the printed PSS-PDDA gels. In brief, gel samples were placed in an Eppendorf tube (Figure 1.b) and briefly washed with PBS solution to remove most of the unbound solute molecules, polymers, and additives. Immediately after the wash, a fresh 1.0 ml of 1X PBS was added to each sample tube (Figure 1.c) and placed capped in 37°C.

After thorough mixing of the supernatant, a 100 μL sample was pipetted each time in a non-treated 96 multiwell Costar[®] plate (Corning Inc., NY, USA) then placed in a SpectraMax M2 microplate reader (Molecular Devices, CA, USA). Liquid samples were excited at 485 nm and fluorescence was measured at 525 nm emission wavelength. Once measured, the same pipette tip was used to aspirate the 100 μL sample from each well and placed back in the Eppendorf tube they were sampled from.

For each solute, fluorescence measurements were then taken after 5, 10, 20, 30, 45, 60 min, then every hour for the first 10 hours, then taken twice a day till day 3 and once a day thereafter. The solute amount in the supernatant at time t , noted M_t , was calculated from the measured fluorescence values using pre-established standard curves. Measurements were carried till M_t reached its maximum, M_{inf} . Fractional release, defined as M_t / M_{inf} , was then calculated and plotted against time to form experimental release profiles. For each solute type and for each PSS:PDDA ion ratio, the reported release profiles and the subsequent diffusion coefficient values were based on a minimum of $N=3$ repeats.

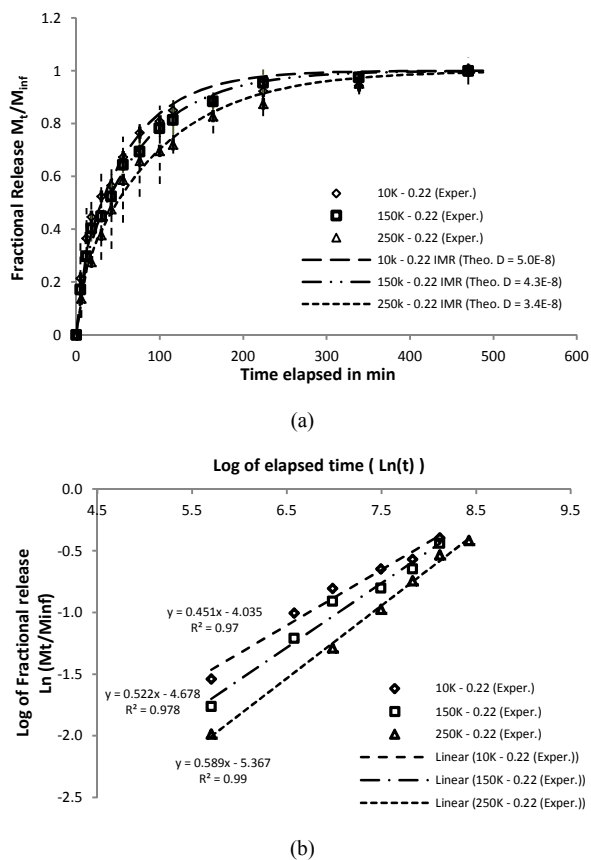


Figure 3. Release profile of FITC-Dextran from printed gels in 1X PBS at 37°C for a target ion mixture ratio (IMR) of 0.22 (2:9). Dextran molecular weights: 10k, 150k, and 250k. (a) Full range fitted with Crank's mode, and (b) Log graph for $M_t/M_{inf} < 0.6$. Note that values plotted in (a) are averages \pm one standard deviation based on $N=3$ repeats.

Model and assumptions

In order to determine the diffusion coefficients from the experimental release profiles, the following assumptions were made. The mass transport of diffusing solutes is release-rate limiting. The diffusion coefficient of the diffusing species is constant. Diffusing substances are homogeneously distributed throughout the printed PSS-PDDA gel samples, i.e. 'monolithic system' conditions. Perfect sink conditions are provided in the release medium during the entire release period. The device is not significantly swelling or swells very rapidly upon contact with physiological buffer and then reaches an equilibrium state. The printed PSS-PDDA gel samples do not erode significantly during solute release. The printed gel samples have plane sheet 'slab' geometry (Figure 2) where diffusion is reduced to one dimension in a medium delimited by two parallel planes²⁶. l is the half-thickness and L the length of the sheet. The film thickness, $2l$, is uniform and equal to the average measured thickness at the swollen state.

Calculation of diffusion coefficient

The mathematical expression used to model the diffusion of FITC-tagged solutes from the printed polyelectrolyte gels is based on Fick's second law expressed in equation (1), where c is the solute concentration at time t and at a distance x away from the center of the plane.

$$\frac{\partial c}{\partial t} = D \frac{\partial^2 c}{\partial x^2} \quad (1)$$

In the case of uniform initial distribution diffusing solutes in plane sheet (slab) geometry, equation (1) is subjected to the following boundary conditions (2) and (3) where C_0 is the initial concentration of diffusing solutes.

$$\text{For } x \text{ between } -l \text{ and } l, \text{ and for } t = 0; \quad C(0) = C_0 \quad (2)$$

$$\text{For } x = -l, x = l, \text{ and for } t > 0; \quad C(t) = 0 \quad (3)$$

Using the separation of variable technique, the solution in the form of trigonometric series of the diffusion equation (1) with the boundary (2) and (3) is expressed in equation (4) (Crank's Model)²⁶.

$$\frac{C_0 - C}{C_0} = 1 - \frac{4}{\pi} \sum_{n=0}^{\infty} \frac{(-1)^n}{2n+1} \exp\left(\frac{-D(2n+1)^2 \pi^2 t}{4l^2}\right) \cos\left(\frac{(2n+1)\pi}{2l} x\right) \quad (4)$$

If M_t denotes the total amount of diffusing solutes that left the sheet at time t , and M_{inf} the corresponding amount after infinite time, equation (5) becomes:

$$\frac{M_t}{M_{inf}} = 1 - \sum_{n=0}^{\infty} \frac{8}{(2n+1)^2 \pi^2} \exp\left(\frac{-D(2n+1)^2 \pi^2 t}{4l^2}\right) \quad (5)$$

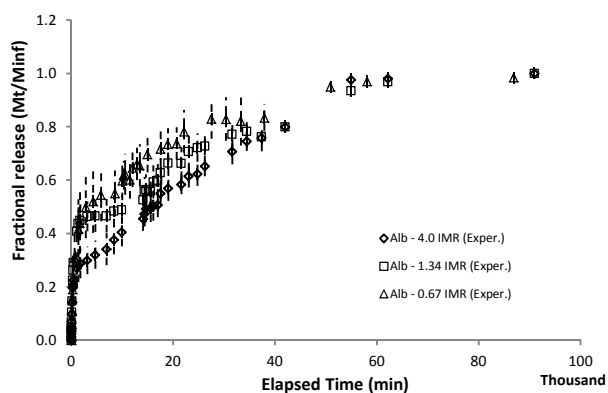
The theoretical values of the fractional release over time were calculated using the first 26 terms of the series in equation (6).

$$\frac{M_t}{M_{inf}} = 1 - \sum_{n=0}^{25} \frac{8}{(2n+1)^2 \pi^2} \exp\left(\frac{-D(2n+1)^2 \pi^2 t}{4l^2}\right) \quad (6)$$

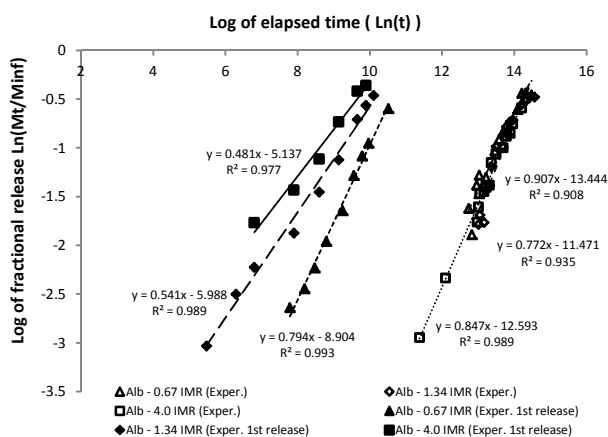
MATLAB version 7.7.0.471 (MathWorks, MA, USA) was used to compute the values and generate the theoretical release profiles. For each sample set, R-squared values were then calculated to find the best fit using curve fitting tool of MATLAB.

Results

For illustration purposes, two sets of profiles are shown respectively in Figures 3.a and 4.a. The first set shows the release profiles of 10k, 150k, and 250k dextran solutes from PSS-PDDA gels printed with 2:9 anion to cation mixture ratio. The second set shows the release profile of albumin from PSS-PDDA gels printed with 0.67 (2:3), 1.34 (4:3), and 4.0 (4:1) anion to cation ratio. The release profile of dextrans shown in Figure 3.a had a single phase characteristic release profile while that of albumin had a two phase, initial and late, release profiles as shown in Figure 4.a. Crank's model was then fitted to the full range of the experimental release profile to calculate the diffusion coefficient in printed gels, noted Dig. The thickness of PSS-PDDA gels studied ranged from 0.2 and 0.5 mm and satisfied the 'slab' geometry assumption where l to L ratio is higher than 10. To help identify the transport mode in printed PSS-PDDA gels, the value of the exponent 'n' of the semi-empirical 'power rule' developed by Ritger-Peppas was determined by plotting the natural log of the fractional release, $\ln(M_t/M_{inf})$, versus the natural log of the elapsed time, $\ln(t)$, then fitted using linear regression as shown in Figure 3.b and 4.b (values M_t/M_{inf} used to were less than 0.6¹⁴). For all reported values in printed PSS-PDDA gels, the goodness of fit (R^2) was above 0.9. The experimental release profiles, Crank's model, and Ritger-Peppas model fitted plots for all other studied solutes and ion mixture ratios can be found in



(a)



(b)

Figure 4. Release profile of FITC-Albumin from printed PSS-PDDA gels in 1X PBS at 37°C for ion mixture ratio of 0.67 (2:3), 1.34 (4:3), and 4.0 (4:1). (a) Full range fitted with Crank's mode, and (b) Log graph for $M_t/M_{inf} < 0.6$ for both initial and late release phases. Note that values plotted in (a) are averages \pm one standard deviation based on $N=3$ repeats.

Limem's work²⁷. The calculated values of D_{ig} for dextran, fluorescein, and albumin in printed PSS-PDDA gels are summarized respectively in Table 1 through 3 and plotted in Figure 5 against the PSS:PDDA ion ratio used. The diffusion of small charged molecules (fluorescein, 0.3 kDa), various size uncharged molecules (dextran, 10 – 250 kDa), and protein (albumin, 67 kDa) in printed PSS-PDDA with near stoichiometric composition (Table 4) occurred respectively at about 10^{-8} , 10^{-9} , and 10^{-10} cm^2/sec . These measured values in printed PSS-PDDA gels is consistent with that reported for PSS-PDDA multilayers made with a classical dipping technique, noted D_{ig} (PEMs)²⁸⁻³⁰.

Discussion

Validity of Fickian diffusion

The calculated values of the diffusion exponent 'n' (Ritger-Peppas) for fluorescein, dextran, and albumin were between 0.41 and 0.91 (Tables 1-3). Based on these values two types of transport are present: Fickian diffusion, i.e. $n \sim 0.5$, and anomalous (non-Fickian) transport, i.e. $0.5 < n < 1$ ¹⁴. For fluorescein and dextrans (Tables 1 and 2) regardless of their

molecular weights, the values of 'n' were between 0.41 and 0.61. The mode of transport is therefore primarily driven by Fickian diffusion. In this case the rate of solute diffusion is much less than that of polymer network relaxation, and hence the transport is diffusion controlled¹⁴. Solute release then follows Fick's law and the estimation of the diffusion coefficient using Crank's model²⁶ is appropriate. As for FITC-Albumin (Tables 3), the values of 'n' were between 0.62 and 0.91, indicating an anomalous type of transport. In this case, the diffusion and relaxation rates are comparable. These concurrent processes make it highly complicated to solve, requiring advanced mathematical treatment or numerical modeling³¹.

Table 1. Calculated diffusion coefficient (D_{ig}) of FITC-Dextran solutes from gels printed with different PSS:PDDA ion ratios in 1X PBS at 37°C.

PSS:PDDA ion ratio	Dextran Size	Fitting with Crank's model (Full range) D_{ig} (cm^2/s)	Fitting with Ritger-Peppas ($M_t/M_{inf} < 0.6$)	
			k	n
2:9 (0.22)	10k	4.9×10^{-8}	0.0177	0.45
	150k	4.3×10^{-8}	0.0093	0.52
	250k	3.4×10^{-8}	0.0047	0.59
1:1 (1.00)	10k	1.4×10^{-8}	0.0063	0.57
	40k	7.4×10^{-9}	0.0042	0.57
4:3 (1.34)	150k	4.7×10^{-9}	0.0057	0.49
	10k	2.4×10^{-8}	0.0197	0.45
4:1 (4.00)	150k	8.7×10^{-9}	0.0168	0.41
	10k	2.5×10^{-8}	0.0038	0.61
	150k	2.7×10^{-8}	0.0061	0.59

Table 2. Calculated diffusion coefficient of Fluorescein from gels printed with 1:1 PSS:PDDA ion ratios in 1X PBS at 37°C.

PSS:PDDA ion ratio	Fitting with Crank's model (Full range) D_{ig} (cm^2/s)	Fitting with Ritger-Peppas ($M_t/M_{inf} < 0.6$)	
		k	n
1:1 (1.00)	1.7×10^{-8}	0.0279	0.61

Table 3. Calculated diffusion coefficient of FITC-Albumin solute from gels printed with different PSS:PDDA ion ratios in 1X PBS at 37°C.

PSS:PDDA ion ratio	Phase of diffusion	Fitting with Crank's model (Full range)		Fitting with Ritger-Peppas ($M_t/M_{inf} < 0.6$)	
		Lag Time (days)	D_{ig} (cm^2/s)	k	n
0.67 (2:3)	Initial	0	2.8×10^{-9}	0.000134	0.79
	Late	4	3.1×10^{-10}	0.000001	0.91
1.00 (1:1)	Initial	0	2.4×10^{-8}	0.001300	0.65
	Late	5	$2.8-5.0 \times 10^{-10}$	0.000200	0.62
1.34 (4:3)	Initial	0	5.9×10^{-9}	0.002508	0.54
	Late	5	4.0×10^{-10}	0.000003	0.85
4.00 (4:1)	Initial	0	9.9×10^{-9}	0.005875	0.48
	Late	5	4.7×10^{-10}	0.000010	0.77

Network properties

One may distinguish between diffusion through water-filled pores and a bulk diffusion mechanism through the homogeneous polymer phase. In water filled pores, the diffusion of solutes is close to their diffusion in pure water, noted D_{iw} , provided that

Table 4. Diffusion coefficients in water (D_{iw}) and in printed PSS-PDDA gels (D_{ig}), hydrodynamic radii (R_H), and molecular weight of fluorescein, dextran, and albumin solutes.

Solute	Shape / charge ⁽ⁱ⁾	Mw (Da)	R_H (nm)	D_{iw} ($\text{cm}^2/\text{s}) \times 10^6$	$D_{ig}^{(ii)}$ (printed) ($\text{cm}^2/\text{s}) \times 10^8$	D_{ig} / D_{iw} (printed)	$D_{ig}^{(iii)}$ (PEMs) ($\text{cm}^2/\text{s}) \times 10^8$
Fluorescein	Small / negative	332	0.4 ⁽³²⁾	3.3 ⁽³³⁾	2.4	0.0072	0.00015 ^(34, 35)
		10,000	2.4 ^(32, 36)	1.1 ⁽³³⁾	1.4	0.0127	N/A
		40,000	5.6 ^(36, 37)	0.71 ⁽³³⁾	0.74	0.0104	N/A
Dextran	Linear/ Non-charged	77,000	7.5 ⁽³⁶⁾	0.26 ⁽²⁹⁾	N/A	N/A	0.6 ^(29, 30)
		150,000	8.8 ⁽³⁸⁾	0.31 ⁽³³⁾	0.43	0.0138	N/A
		Albumin	Globular / negative	67,000	3.1 ⁽³⁹⁾	0.51-0.73 ^(33, 40, 41)	0.03-0.05

(i) Charge under physiological pH.

(ii) Diffusion coefficients as measured in printed PSS-PDDA made with stoichiometric ratio of cations and anions.

(iii) Diffusion coefficient as reported in the literature of solutes in PSS-PDDA polyelectrolyte multilayers made with classical dipping technique.

they have a similar or smaller size than the pore, i.e. $D_{iw}/D_{ig} \sim 1$. In the bulk however, solute transport is slowed down significantly due to the obstructing effect of polymer chains, i.e. $D_{iw}/D_{ig} \ll 1$. Based on the results, shown in Table 4, dextran diffusion was significantly slowed for molecular weights equal or higher than 10kDa ($D_{iw}/D_{ig} \sim 0.01$). On the other hand, PSS-PDDA non-annealed multilayers were permeable to low molecular dextrans (Mw 4,400) ³⁰. The characteristic pore (mesh) size ξ of the polyelectrolyte complex printed with near stoichiometric ratio is then between the hydrodynamic radius of 4.4 kDa and 10 kDa dextrans, i.e. between 1.9 and 2.4 nm. With reference to the classification of hydrogels based on porosity-related swelling kinetics where $1 \leq \xi < 10$ nm ³², the printed PSS-PDDA complexes are non-porous homogenous hydrogels. It should also be noted that the pore size depends on the nature of the polyelectrolyte pair and the fabrication conditions used (annealed versus non-annealed). The smallest reported pore sizes were between 0.4 and 0.5 nm for PSS/PAH annealed multilayers ⁴².

Effect of solute size

With the classical understanding of polymer network in chemical hydrogels, one would expect that solutes with a radius larger than the mesh size would not be released out of the gel, much like large fish trapped inside a tight fishing net where the knots represent the covalent bonds crosslinking adjacent polymer chains. Some examples of these chemical gels are chitosan gels crosslinked with glutaraldehyde ⁴³, Poly(4-vinylpyridine) cross-linked with alkyl dihalide ⁴⁴, and acrylate gels. These gels found application as separation membranes where the characteristic mesh size, ξ , of the crosslinked network acted as a cut-off line for macromolecules with sizes larger than ξ ^{43, 44}. A frequently used model to describe this restricting effect is the Renkin ⁴⁵ model assumes that solutes are spheres passing through cylindrical pores. For a complete picture of the restrictive effect of chemical hydrogel, solute geometry should also be taken into account ⁴⁶. Typical examples studied included proteins (e.g. albumin, cytochromes, etc.) and dextrans. Proteins represent hard globular solutes while dextrans are random coil flexible polymers ⁴⁷. Following the models of DeGennes and Edwards for polymer diffusion, as linear chains dextrans will reptate through the gel network much faster than would be possible for rigid spherical

molecules of similar molecular weight ^{46, 48}.

In other words, the molecular cut-off in a given chemical gel (fixed ξ) is higher for flexible polymers compared to that of hard globular solutes, which is consistent with the faster release rates reported in Table 4 of dextrans versus albumin.

As for albumin, it should first be noted that the measured initial release was about hundred times faster than late release and consistent with the measured release rates of fluorescein. This observation indicates that the initial release observed in the FITC-albumin profile is likely dominated by the presence of loose FITC in the printed complex followed by the characteristic release of albumin at about 10^{-10} cm^2/sec . Second, the size of albumin ($R_H = 3.1$ nm) was larger than the estimated mesh size of printed PSS-PDDA (~ 2 nm), yet it still diffused out of the gel. Therefore, it is unlikely that polyelectrolyte complexes are gels with set distance between crosslinks, i.e. ‘fixed’ mesh size ξ , and rather confirms that they are ‘living systems’ ⁴⁹ very sensitive to changes in their environment. They undergo continuous internal reorganization of charge ⁵⁰ and should rather be treated as ‘viscous fluids’ ⁵¹ held together via transient ‘junction zones’ ⁵². Instead of a fish net, printed polyelectrolyte gels should rather be pictured as a noodle plate with mixed vegetables inside. Regardless of the size, polyelectrolyte chains (noodles) rearrange themselves to allow the passage of the solutes (vegetables). The rate at which this passage occurs depends greatly on the nature of the solute (shape, size, and charge) and the nature of the polyelectrolyte pair. Strong polyelectrolytes (high charge density) would act like overcooked noodles where the chains are sticky and rearrangement takes longer, whereas weak polyelectrolyte would be less sticky and rearrange faster.

Effect of solute charge

As listed in Table 4, the diffusion coefficient of Albumin (MW = 67 kDa, globular shape molecule with an overall negative charge at physiological pH, and $R_H = 3.5$ nm, measured $D_{ig} \sim 4 \times 10^{-10}$ cm^2/s) was one order of magnitude slower than that of 77 kDa dextran (linear uncharged, $R_H = 7.5$ nm, $D_{ig} \sim 6 \times 10^{-9}$ cm^2/s). The measured diffusion coefficients of albumin in slowly printed PSS-PDDA complexes were in the same range as that measured in PSS-PAH multilayer capsules ²⁸. These results are also consistent with the diffusion of other proteins (e.g. Avidin) ⁵³ and

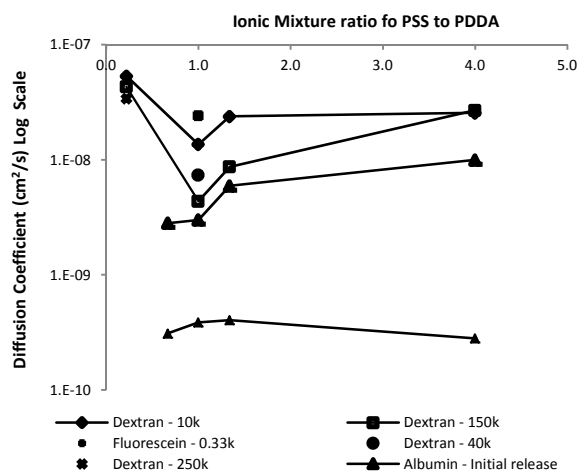


Figure 5. Effect of the PSS:PDDA ion ratio on the diffusion coefficient of Fluorescein, Albumin and 10k, 40k, 150k, and 250k Dextran solutes in printed gels in 1X PBS at 37°C.

zwitterionic molecules in general at about 10^{-10} cm^2/s ^{54, 55}. These studies demonstrate the existence of an electrostatic drag resulting from the electrostatic interaction between the charged solutes and the surrounding polyelectrolyte complex.

5 Effect of gel stoichiometry

The release profiles of albumin (Figure 4.a) were distinct from those of dextrans (Figure 3.a). All dextran release profiles displayed a single phase release with a characteristic diffusion coefficient ranging from 0.4 to 4.9×10^{-8} cm^2/sec . However, albumin release occurred in two phases: initial and late releases. The initial release happened at rates between 0.3 to 2.8×10^{-8} cm^2/sec while late release took place at rates between 2.8 and 4.7×10^{-10} cm^2/sec (Tables 4). Based on these results, the initial release of albumin occurred roughly at similar rates as those of dextrans. Second, the initial release of albumin showed a strong dependence on the stoichiometry of the printed gel sample (Figure 5). Release was slowest (0.3×10^{-8} cm^2/sec) from gels printed with excess positive charge, i.e. PDDA, compared to stoichiometric gel samples (1.0×10^{-8} cm^2/sec). Third, the late release of albumin was independent from the initial printed gel stoichiometry (Table 4 and Figure 5).

The slower release of albumin from gels printed with PSS:PDDA ion ratio of 0.67 (excess positive charge) can be explained by the electrostatic interaction between the negatively charged albumin at physiological pH and the excess PDPA. On the other hand, the similarities between albumin release rates in the late phase indicate that the environment surrounding the diffusing solute (albumin) in the various samples is rather similar. Therefore, gel samples must have changed over time and can be understood in the light of the compositional change discussed in our previous work⁸. Given this consideration, PSS-PDPA gels originally printed with different polyelectrolyte ratios caused albumin to diffuse out with distinct rates in the initial phase. Concurrently, excess polymer is also diffusing out of the non-equilibrium complex. At the end of the initial phase (release), all PSS-PDPA gels reach a near-stoichiometric ratio composition (equilibrium state) beyond which albumin diffused out at similar rates. It can be further deduced that the rearrangement (diffusion) rate of

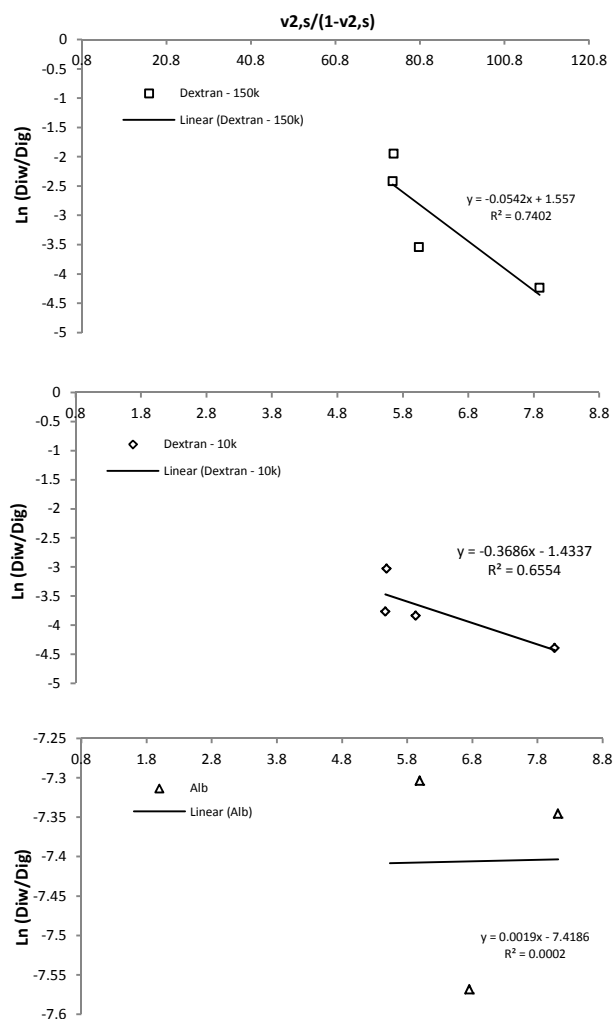


Figure 6. Applicability of free volume theories to solute transport in PSS-PDPA printed gels.

polyelectrolyte chains in non-stoichiometric gels is in the order of 10^{-8} cm^2/sec .

This analysis is in agreement with polyelectrolyte multilayer literature. In fact, in HA/PLL multilayers, some chains appeared fixed at the time scale of fluorescence recovery after photobleaching experiments (diffusion coefficient $< 10^{-11}$ cm^2/sec), whereas there exists a population of slowly diffusing polyions (diffusion coefficient $\approx 10^{-10}$ cm^2/sec) and a third population of rapidly diffusing chains (diffusion coefficient $\approx 10^{-8}$ cm^2/sec)⁵⁶. The first population consists of the fully complexed polyelectrolyte chains. The second corresponds to chains in partial electrostatic interaction with the complex (in accord with the release rate of albumin in our experiments). The third represents excess polymer chains having minimal interaction with the complex.

Applicability of classical transport theories

For homogenous gels composed of flexible polymer chains²⁵, the hydrodynamic and free-volume theories may be applicable. The hydrodynamic-scaling model described best the diffusion of solutes in homogeneous hydrogels; however, it suffers from

containing an undefined polymer solvent interaction parameter, k_c ,²⁵. On the other hand, free volume models⁵⁷ are more frequently used even in the polyelectrolyte multilayer literature³⁰. Nonetheless, they are typically applied to situations for which the assumptions made in their derivation are not valid and are not physically consistent²⁵. To further confirm the limitation of these models in the case of polyelectrolyte complexes, the free volume model was applied to the printed PSS-PDDA gels and results shown in Figure 6. Based on the model, the relation between the natural log of (D_{ig}/D_{iw}) and $v_{2,s}/(1-v_{2,s})$ should be linear as expressed in equation (7), where $v_{2,s}$ is the polymer volume fraction in the swollen state, k_2 is a constant describing the polymer-solvent interaction, and ψ is a factor accounting for the sieving effect of the gel^{32,33}.

$$\ln\left(\frac{D_{ig}}{D_{iw}}\right) = \ln(\psi) - k_2 R_H^2 \left(\frac{v_{2,s}}{1-v_{2,s}}\right) \quad (7)$$

The plots in Figure 6 show weak linear correlations ($R^2 \sim 0.7$) for dextrans and no correlation for albumin ($R^2 \sim 0$). Based on these results, it may be argued that the free volume theory gives a fair description of the transport of non-charged molecules. However it is not applicable in the case of charged solutes. The model lacks a component to account for the interaction between charged solutes and the charged polyelectrolyte chains. This interaction increases the drag on solutes hence resulting in slower diffusion rates. Furthermore, the time-dependent composition of ionic self-assembled polyelectrolyte gels, notably for non-stoichiometric gels, makes modeling a more challenging task.

Furthermore, the time-dependent composition of ionic self-assembled polyelectrolyte gels, notably for non-stoichiometric gels, makes modeling a more challenging task. While the fluorescein, dextrans and albumin all show Fickian diffusion, it would be expected that some diffusants will bind to one of the gel components and show non-Fickian behavior.

Conclusion

Solute transport in the bulk of printed polyelectrolyte complexes occurs primarily through Fickian diffusion. The diffusion coefficients of small molecules ($R_H < 1$ nm), various size uncharged molecules ($2.4 \leq R_H \leq 8.8$ nm), and protein (albumin, $R_H \leq 3.1$ nm) in printed complexes were respectively in the order of 10^{-8} , 10^{-9} , and 10^{-10} cm²/sec. The often used free volume was found applicable to model the transport of uncharged molecules in printed polyelectrolyte complexes. However, this model falls short in the case of charged molecules due to the lack of a term describing the electrostatic drag imparted on solutes by the surrounding polyions. Polyelectrolyte complexes are “living systems” very sensitive to changes of their environment. They undergo continuous internal reorganization of charge⁵⁰. Unlike chemical gels, polyelectrolyte complexes should be treated as ‘viscous fluids’⁵¹ held together via transient ‘junction zones’⁵². The apparent mesh size ξ in near stoichiometric composition was estimated to about 2 nm.

Acknowledgement

The research carried out at University of Massachusetts Dartmouth was supported through grants from the National

Textile Center and from the NIH through the Tissue Engineering Resource Center (TERC) at Tufts University. Authors would like to thank Dr. Chen Lu Yang (Advanced Manufacturing and Technology Center at the University of Massachusetts Dartmouth) and Dr. David Kaplan (Tufts University) for their support.

Notes and references

- ^a Department of Bioengineering, University of Massachusetts Dartmouth, North Dartmouth, MA - USA. Fax: 508.999.9139; Tel: 508.415.7110; E-mail: limem.skander@gmail.com
- ^b Department of Chemical Engineering, New Mexico Tech, Socorro, NM - USA. Tel: 575.835.5210; E-mail: pcalvert@nmt.edu
- G. Decher, *Science*, 1997, **277**, 1232-1237.
 - G. Decher, J. D. Hong and J. Schmitt, *Thin Solid Films*, 1992, **210**, 831-835.
 - J. Cho, K. Char, J.-D. Hong and K.-B. Lee, *Adv. Mater.*, 2001, **13**, 1076-1078.
 - A. Izquierdo, S. S. Ono, J. C. Voegel, P. Schaaf and G. Decher, *Langmuir* 2005, **21**, 7558.
 - J. B. Schlenoff, S. T. Dubas and T. Farhat, *Langmuir*, 2000, **16**, 9968-9969.
 - A. H. Rmaile, Florida State University, Tallahassee, 2007.
 - K. C. Krogman, N. S. Zacharia, S. Schroeder and P. T. Hammond, *Langmuir*, 2007, **23**, 3137-3141.
 - S. Limem, D. McCallum, G. G. Wallace, M. In Het Panhuis and P. Calvert, *Soft Matter*, 2011, **7**, 3818-3826.
 - C. M. Andres and N. A. Kotov, *J. Am. Chem. Soc.*, 2010, **132** 14496-14502.
 - F. Siepmann, J. Siepmann, M. Walther, R. J. MacRae and R. Bodmeier, *J. Control. Rel.*, 2008, **125**, 1-15.
 - B. V. Slaughter, S. S. Khurshid, O. Z. Fisher, A. Khademhosseini and N. A. Peppas, *Adv. Mater.*, 2009, **21**, 3307-3329.
 - D. Y. Arifin, L. Y. Lee and C.-H. Wang, *Adv. Drug Deliv. Rev.*, 2006, **58** 1274-1325.
 - C. C. Lin and A. T. Metters, *Adv. Drug Delivery Rev.*, 2006, **58**, 1379-1408.
 - P. L. Ritger and N. A. Peppas, *J. Control. Rel.*, 1987, **5**, 23-36.
 - J. Siepmann and F. Siepmann, *J. Contr. Rel.*, 2012, **161**, 351-62.
 - Y. N. Kalia and R. H. Guy, *Adv. Drug Deliv. Rev.*, 2001, **48** 159-172.
 - S. R. Van Tomme, B. G. Geest, K. Braeckmans, S. C. De Smedt, F. Siepmann, J. Siepmann, C. F. Van Nostrum and W. E. Hennink, *J. Control. Rel.*, 2005, **110**, 67-78.
 - N. A. Peppas, J. Zach Hilt, A. Khademhosseini and R. Langer, *Adv. Mater.*, 2006, **18**, 1345-1360.
 - S. H. Gehrke, J. P. Fisher, M. Palais and M. E. Lund, *Annal. New York Acad. Sci.*, 1997, **831**, 179-184.
 - N. A. Peppas and A. R. Khare, *Adv. Drug Deliv. Rev.*, 1993, **11**, 1-35.
 - L. F. Gudeman and N. P. Peppas, *J. Membr. Sci.*, 1995, **107**, 239-248.
 - R. J. Phillips and J. F. Brady, *J. Colloid. Interf. Sci*, 1990, **139**, 363-373.
 - T. Stylianopoulos, B. Diop-Frimpong, L. L. Munn and R. K. Jain, *Biophys J.*, 2010, **99**, 3119-3128.
 - J. S. Vrentas and J. L. Duda, *AIChE J.*, 1979, **25**, 1-24.
 - B. Amsden, *Macromol.*, 1998, **31**, 8382-8395.

26. J. Crank, *Mathematics of Diffusion*, 1975.
27. S. Limem, in *Department of Bioengineering*, University of Massachusetts Dartmouth, 2013, pp. 162-173.
28. L. Szyk, P. Schwinte, J. C. Voegel, P. Schaad and B. Tinland, *J. Phys. Chem. B.*, 2002, **106**, 6049-6055.
29. T. Adalsteinsson, W.-F. Dong and M. Schönhoff, *J. Phys. Chem. B.*, 2004, **108**, 20056-20063.
30. Y. Qiao, P. Galvosas, T. Adalsteinsson, M. Schonhoff and P. T. Callaghan, *J. Chem. Phys.*, 2005, **122**, 214912-1-9.
31. C. Yin and X. Li, *Inter. J. Pharm.*, 2011, **10**, 78-87.
32. A. Ekani-Nkodo and D. K. Kuchnir Fyngenson, *Phys. Rev. E.*, 2003, **67**, 021909
33. R. L. Mauck, C. T. Hung and G. A. Ateshian, *J. Biomech. Eng.*, 2003, **125**, 602-614.
34. G. Ibarz, L. Dähne, E. Donath and H. Möhwald, *Chem. Mater.*, 2002, **14**, 4059-4062.
35. A. A. Antipov, G. B. Sukhorukov and E. Donath, *J. Phys. Chem. B.*, 2001, **105** 2281-2284.
36. L. Lebrun and G. A. Junter, *Enzym. Microb. Technol.*, 1993, **15**, 1057-1062.
37. W.-F. Dong, J. K. Ferri, T. Adalsteinsson, M. Schönhoff, G. B. Sukhorukov and H. Möhwald, *Chem. Mater.*, 2005, **17**, 2603-2611.
38. B. Amsden, *Polymer*, 2002, **43**, 1623-1630.
39. M. T. Tyn and T. W. Gusek, *Biotechnol. Bioeng.*, 1990, **35**, 327-338.
40. A. Shkilnyy, P. Proulx, J. Sharp, M. Lepage and P. Vermette, *Colloid. Surf. B: Biointerf.*, 2012, **93**, 202-207.
41. J. V. Nauman, P. G. Campbell, F. Lanni and J. L. Anderson, *Biophys. J.*, 2007, **92**, 4444-4450.
42. X. Liu and M. L. Bruening, *Chem. Mater.*, 2004, **16**, 351-357.
43. B. Krajewska and A. Olech, *Polym. Gels Netw.*, 1996, **4**, 33-43.
44. Q. Wang, S. Samitsu and I. Ichinose, *Adv. Mater.*, 2011, **23**, 2004-2008.
45. E. M. Renkin, *J. Gen. Physiol.*, 1954, **38**, 225-243.
46. S. Mochizuki and A. Zydney, *J. Membr. Sci.*, 1992, **68**, 21-41.
47. J. A. M. Smit, J. A. A. P. Van Dijk, M. G. Mennen and M. Daoud, *Macromol.*, 1992, **25**, 3585-3590.
48. J. Noolandi, S. G. W, H. A. Lim and J. L. Viovy, *Science*, 1989, **243**, 1456-1458.
49. A. F. Thünemann, M. Müller, H. Dautzenberg, J. F. Joanny and H. Löwen, *Adv. Pym. Sci.*, 2004, **166**, 113-171.
50. T. R. Farhat and J. B. Schlenoff, *J. Am. Chem. Soc.*, 2003, **125**, 4627-4636.
51. K. Kohler, P. M. Biesheuvel, R. Weinkamer, H. Mohwald and G. B. Sukhorukov, *Phys. Rev. Lett.*, 2006, **97**, 188301/1-4.
52. S. B. Ross-Murphy, *Polym. Gels Netw.*, 1994, **2**, 229-237.
53. Y. Endo, K. Sato and J. I. Anzai, *Polym. Bull.*, 2011, **66**, 711-720.
54. R. Von Klitzing and H. A. Mohwald, *Macromol.*, 1996, **29**, 6901-6906.
55. L. Wang, M. Schönhoff and H. Möhwald, *J. Phys. Chem. B.*, 2004, **108**, 4767-4774.
56. C. Picart, J. Mutterer, Y. Arntz, J.-C. Voegel, P. Schaaf and B. Senger, *Microsc. Res. & Tech.*, 2005, **66**, 43-57.
57. F. Ganji, S. Vasheghani-Farahani and E. Vasheghani-Farahani, *Iran. Polym. J.*, 2010, **19**, 375-398.